PERGAMON

International Journal of Solids and Structures 38 (2001) 9347–9357

INTERNATIONAL JOURNAL OF SOLIDS and STRUCTURES

www.elsevier.com/locate/ijsolstr

Semiactive control of a shape memory alloy hybrid composite rotating shaft

A. Tylikowski [a], R.B. Hetnarski [b,*]

[a] *Institute of Machine Design Fundamentals, Warsaw University of Technology, 02-524 Warszawa, Narbutta 84, Poland*

[b] *Department of Mechanical Engineering, James E. Gleason Building, Rochester Institute of Technology, 78 Partridge Hill, Honeoye Falls, Rochester, NY 14623, USA*

Received 28 December 1999

Abstract

In this paper the technique of the dynamic stability analysis proposed for the conventional laminated structures is extended to the activated shape memory alloy (SMA) hybrid rotating shafts under the time-dependent compressive axial loading. The influence of the activation through the change of the temperature on the dynamic stability domains is examined. Changing with the temperature the Young's modulus of SMA fibers enters into a global stiffness parameter of the shaft. Thermally induced membrane forces in SMA fibers and changing with temperature damping coefficient also modify shaft dynamic equations. The activated SMA hybrid shaft is treated as a beam-like structure. The thin-walled composite shaft is flexible thus it should be supported on the both ends in order to avoid large deflections. By using the standard stability technique we arrive at the effective sufficient criterion of the dynamic and almost sure stochastic stability. The stability regions are given as functions of the loading characteristics, the external damping coefficient, the lamination angle, and the properties of the shaft material. The results indicate that the global activation causes an increase of the critical (admissible) axial force both for the glass–epoxy/NiTi–epoxy and for the graphite–epoxy/NiTi–epoxy hybrid shafts. © 2001 Elsevier Science Ltd. All rights reserved.

Keywords: Dynamic stability; Rotating shaft; Liapunov method; Hybrid composites; Semiactive control

1. Introduction

Recently, composite materials find an increased range of applications for high-performance rotating shafts (e.g., see Nepershin and Klimov, 1986; Bauchau, 1983). Thin-walled standard angle-ply laminated tubes meet relatively easy the requirements of torsional strength and stiffness but are more flexible to bending and have specific elastic and damping properties which depend on the system geometry, on the physical properties of plies, and on the laminate arrangement. Such systems are also sensitive to lateral buckling.

* Corresponding author. Tel.: +1-716-582-2799; fax: +1-716-475-7710.
E-mail address: 632hetna@rit.edu (R.B. Hetnarski).

PII: S0020-7683(01)00086-5

The shape memory alloy (SMA) hybrid composites are a class of materials capable of changing both their stiffnesses through the application of in-plane loads and their elastic properties. The stiffness modification occurs as a result of the thermally induced martensite phase transformation of the SMA fibers which are embedded in standard laminated composite structures. The shape memory effect may be described as follows. An element in the low-temperature martensitic condition, when it is plastically deformed and then the external load is removed, will regain its original shape when heated. The variation of the Young's modulus of the SMA is very different from that of conventional metallic materials. The Young's modulus of the nitinol (Nickel–titanium alloys), which is an example of such a material, increases 3–4 times (Cross et al., 1970), when the temperature changes from that below M_{f} (i.e., in the martensite phase) to that above A_{f} (i.e., in the austenite phase). A nitinol of proper composition exhibits unique mechanical memory or restoration force characteristics. Large plastic strains of the magnitude of 6–8% may be completely removed by the process of heating the material so as to transform it to its austenite phase. The damping of vibrations in the SMA due to internal friction exhibits also an important characteristics. The low-temperature martensic phase is characterized by a large damping coefficient while the high-temperature austenitic phase shows a low damping coefficient. The decrease ratio is approximately equal to 1:10 (Dejonghe et al., 1977). Comprehensive studies of eigenfrequencies and eigenfunctions of the SMA hybrid adaptive panels with uniformly and piecewise distributed actuation have been presented in papers by Rogers (1990), Rogers et al. (1990) and Pietrzakowski (2000). The results indicate that the activation by the temperature effectively changes the eigenfrequencies, the mode shape of the plate, and the sound transmission through composite panels.

In this paper the technique of the dynamic stability analysis proposed for the conventional laminated structures is extended to the activated SMA hybrid structures under the axial time-dependent loads. In this dynamics study the hybrid elements will be treated as a thin symmetrically laminated shell containing both the conventional (e.g., graphite or glass) fibers, and the activated SMA fibers. As the dynamic stability problem is related to the parametric vibration of structures, the stabilization of motion strongly depends on a dissipation of energy. The commonly used simplest model of viscous damping with constant coefficients is assumed in the paper, despite the fact that there exist more advanced theories of energy dissipation (see Schultz and Tsai, 1969). Formulas determining the dynamic stability regions will be written explicitly, and the parameters of stability domains will be calculated.

The purpose of the paper is to analyze the stability criterion of the shaft equilibrium. We will consider the influence of the activation through the change of the temperature on the stability domains of the shaft in the case when the axial force is time-dependent. The stochastic loading is assumed in the form of the ergodic stationary processes, with continuous realizations. The structure buckles dynamically when the axial force becomes so large that the structure does not oscillate about the unperturbed state, and a new increasing mode of oscillations occurs. In order to estimate the perturbed structure motions we introduce a measure of distance, $\|\cdot\|$, of the solution of dynamics equations with nontrivial initial conditions from the trivial solution. We say that the trivial solution $w = 0$ of dynamics equations is almost sure asymptotically stable if the measure of distance between the perturbed solution and the trivial solution, $\|\cdot\|$, satisfies the condition $P(\lim_{t\to\infty} \|w(.,t)\| = 0) = 1$, where P denotes the probability. Using the appropriate energy-like Liapunov functional, the sufficient stability conditions for the almost sure stochastic stability of the shaft equilibrium are derived. Finally, the influence of SMA activation on stability regions is examined.

2. Activated rotating shafts

The shaft, treated as a symmetrically laminated shell, contains both the conventional (e.g., graphite or glass) fibers oriented at $+\Theta$ and $-\Theta$ to the shell axis and the activated SMA fibers parallel to the shaft axis (cf. Fig. 1). The SMA fibers are placed in sleeves. If the ends of fibers are fixed to the external frames the

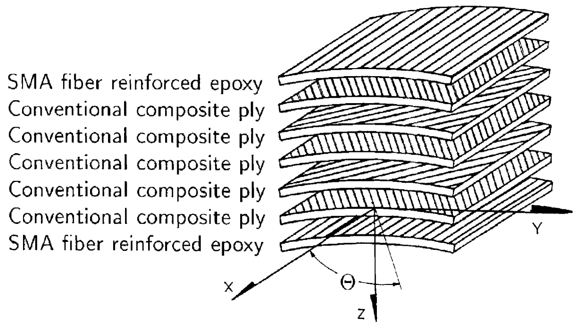

Fig. 1. Exploded view of the shaft layers.

recovery stresses generate the tensile axial force in the shaft. If the ends of SMA fibers are fixed to the shaft hoops, the recovery stresses are balanced by the shaft, and the resultant axial force in the shaft cross-section is equal to zero. The shaft, which rotates with constant angular velocity Ω, is also subjected to a constant or time-dependent external axial destabilizing force $S(t)$. Due to the symmetric arrangement of layers, the equations relating in-plane moments and force resultants with the strain state components decouple, and we can write the constitutive equation of a symmetrically laminated tube (since the coupling stiffness matrix B is equal to zero, cf. Jones, 1975) in the form

$$\begin{bmatrix} N_{11} \\ N_{22} \\ N_{12} \end{bmatrix} = \begin{bmatrix} A_{11} & A_{12} & A_{16} \\ A_{12} & A_{22} & A_{26} \\ A_{16} & A_{26} & A_{66} \end{bmatrix} \begin{bmatrix} \epsilon_{11} \\ \epsilon_{22} \\ \epsilon_{12} \end{bmatrix} \tag{1}$$

where ϵ_{ij} and A_{ij} denote strains and in-plane laminate stiffness matrix, respectively. Assuming that the shaft consists of a large number of orthotropic layers, A_{16} and A_{26} become negligible and the matrix equation (1) decouples. Since the circumferential force N_{22} is much smaller than the axial force, we may neglect N_{22} in the second equation of Eq. (1) and calculate the reduced Young's modulus of the beam-like cylindrical shell (Bauchau, 1983)

$$E_0 = \left(A_{11} - \frac{A_{12}^2}{A_{22}} \right) \frac{1}{h} \tag{2}$$

Changing with temperature Young's modulus enters into the stiffness matrix, where in-plane shell stiffnesses are expressed by

$$A_{ij} = \sum_{k=1}^{N} (\bar{Q}_{ij})_k h_k \tag{3}$$

The reduced stiffnesses $\bar{Q}_{ij}$ of the kth layer of thickness h_k can be calculated using the engineering constants of orthotropic layer E_{11}, E_{22}, G_{12}, v_{12}, and the lamination angle Θ.

By forcing the martensite austenite transformation of the SMA layer we modify the basic mechanical properties, such as the Young's modulus and the internal damping coefficient. Also, we apply the recovery stresses which partially act in the cross-section of the shaft, and partially are balanced by the shaft boundaries. The shaft is compressed by an external force consisting of a constant value F_0 and the variable part $F(t)$. The shaft of length ℓ is assumed to have a constant circular cross-section without initial geometrical imperfections. The mean density is denoted by ρ and the area and the geometrical moment of inertia of the shaft's cross-section are denoted by A and J, respectively. The dynamic equations, containing the Coriolis acceleration and the acceleration of transportation, are written in the rotating coordinate system with respect to displacements u and v of the shaft axis. A viscous model of external damping with a constant proportionality coefficient β and the Voigt–Kelvin model of internal damping with the coefficient λ are assumed to describe the dissipation of the shaft energy. The equations of motion of the shaft, expressed by transverse displacements u and v in the movable coordinate system (y, z), has the form

$$u_{,tt} - \Omega^2 u + 2\Omega v_{,t} + \beta(u_{,t} + \Omega v) + eu_{,xxxx} + \lambda u_{,xxxxt} + (f_0 + f(t))u_{,xx} = 0, \quad x \in (0, \ell) \tag{4}$$

$$v_{,tt} - \Omega^2 v - 2\Omega v_{,t} + \beta(v_{,t} - \Omega u) + ev_{,xxxx} + \lambda v_{,xxxxt} + (f_0 + f(t))v_{,xx} = 0 \tag{5}$$

where $e = E_0 J/\rho A$, $f_0 = F_0/\rho A$, $f(t) = F(t)/\rho A$ and Ω is the angular velocity. Due to the small thickness, the shaft is flexible and smooth working conditions require support at both ends. It means that the displacements of the shaft in supporting bearings are small as compared with the transverse displacements of thin-walled flexible shaft. Thus, we have the following boundary conditions expressed in terms of displacements

$$\begin{aligned} &u(0,t) = v(0,t) = 0, \quad u_{,xx}(0,t) = v_{,xx}(0,t) = 0 \\ &u(\ell,t) = v(\ell,t) = 0, \quad u_{,xx}(\ell,t) = v_{,xx}(\ell,t) = 0 \end{aligned} \tag{6}$$

3. Stability analysis

In order to derive the dynamic stability criteria the Liapunov functional is applied in a form of a sum of the modified kinetic energy and the elastic energy of the shaft (cf., Tylikowski, 1986)

$$\begin{aligned} \mathscr{V} = \frac{1}{2}\int_0^\ell \Big\{ &(u_{,t} + \Omega v + \beta u + \lambda u_{,xxxx})^2 + (u_{,t} + \Omega v)^2 + (v_{,t} - \Omega u + \beta v + \lambda v_{,xxxx})^2 + (v_{,t} - \Omega u)^2 \\ &+ 2e(u_{,xx}^2 + v_{,xx}^2) + 2f_0(u_{,x}^2 + v_{,x}^2) \Big\} \mathrm{d}x \end{aligned} \tag{7}$$

The functional (7) is positive-definite if the axial force f_0 is smaller than the static buckling load f_{cr}. Then the measure of distance can be chosen as a square root of the functional $\|w(x,t)\| = \mathscr{V}^{1/2}$. First we analyze the case of constant axial loading $f(t) = 0$. As the force f_0 acting in the shaft axis is constant, the classic differentiation rule is applied in order to calculate the time derivative of the functional in the direction of the shaft motion

$$\begin{aligned} \frac{\mathrm{d}\mathscr{V}}{\mathrm{d}t} = -\beta \int_0^\ell \Big\{ &(u_{,t}^2 + v_{,t}^2) + \lambda(u_{,xxt}^2 + v_{,xxt}^2) + \lambda e(u_{,xxxx}^2 + v_{,xxxx}^2) + (\beta e - \Omega^2)(u_{,xx}^2 + v_{,xx}^2) \\ &- \lambda f_0(u_{,xxx}^2 + v_{,xxx}^2) + 2\Omega\beta(u_{,t}v - uv_{,t}) - \beta f_0(u_{,x}^2 + v_{,x}^2) + \beta\Omega^2(v^2 + u^2) \Big\} \mathrm{d}x \end{aligned} \tag{8}$$

After rewriting, we receive

$$\frac{\mathrm{d}\mathscr{V}}{\mathrm{d}t} = -\beta\mathscr{V} + \mathscr{U} \tag{9}$$

where the auxiliary functional $\mathscr{U}$ is known. Now, we look for a function χ which satisfies the following inequality

$$\mathscr{U} \leqslant \chi\mathscr{V} \tag{10}$$

Substituting the inequality (10) into Eq. (9) yields the first order differential inequality

$$\frac{\mathrm{d}\mathscr{V}}{\mathrm{d}t} \leqslant (\chi - \beta)\mathscr{V} \tag{11}$$

the solution of which is given as

$$\mathscr{V}(t) \leqslant \mathscr{V}(0)\exp\left[-\left(\beta - \frac{1}{t}\int_0^t \chi(\tau)\mathrm{d}\tau\right)t\right] \tag{12}$$

Using inequality (12) we obtain the upper estimation of the measure of distance between the disturbed solution and the trivial solution

$$\|w(x,t)\| \leqslant \|w(x,0)\|\exp\left[-\frac{1}{2}\left(\beta - \frac{1}{t}\int_0^t \chi(\tau)\mathrm{d}\tau\right)t\right] \tag{13}$$

Sufficiently large damping coefficient β implies the stability of equilibrium state.

In order to find χ effectively we use the expansions of the displacement satisfying boundary conditions (6)

$$u(x,t) = \sum_{n=1}^{\infty} S_n(t)\sin\frac{n\pi x}{\ell} \tag{14}$$

$$v(x,t) = \sum_{n=1}^{\infty} T_n(t)\sin\frac{n\pi x}{\ell} \tag{15}$$

Therefore,

$$u_{,t}(x,t) = \sum_{n=1}^{\infty} \dot{S}_n(t)\sin\frac{n\pi x}{\ell} \tag{16}$$

$$v_{,t}(x,t) = \sum_{n=1}^{\infty} \dot{T}_n(t)\sin\frac{n\pi x}{\ell} \tag{17}$$

Due to the existence of even-order space derivatives in the functional (7) and in its time-derivative (8), the value of functionals can be calculated as a sum of the suitable quadratic terms

$$\mathscr{V} = \sum_{n=1}^{\infty} \mathscr{V}_n \tag{18}$$

$$\mathscr{U} = \sum_{n=1}^{\infty} \mathscr{U}_n \tag{19}$$

where $\mathscr{V}_n$ is calculated from formula (7) for a single term of the expansion. If χ_n, which satisfies a single term inequality, is known

$$\frac{\mathrm{d}\mathscr{V}_n}{\mathrm{d}t} + \beta\mathscr{V}_n = \mathscr{U}_n \leqslant \chi_n\mathscr{V}_n \tag{20}$$

then the following chain of inequalities is true

$$\mathscr{U} = \sum_{n=1}^{\infty} \mathscr{U}_n \leqslant \sum_{n=1}^{\infty} \chi_n\mathscr{V}_n \leqslant \left(\max_{n=1,2,\ldots} \chi_n\right)\mathscr{V} = \chi\mathscr{V} \tag{21}$$

Therefore, the function χ can be effectively calculated. Introducing $\kappa_n = \chi_n - \beta$ we rewrite inequality (20) in the form

$$\kappa_n \mathscr{V}_n - \frac{\mathrm{d}\mathscr{V}_n}{\mathrm{d}t} \geqslant 0 \tag{22}$$

Substituting the nth terms of expansions (14)–(17) into inequality (22) we obtain the second order quadratic inequality with respect to the four variables T_n, $\dot{T}_n$, S_n, $\dot{S}_n$:

$$\begin{aligned} &\bigg[\dot{S}_n^2 + T_n^2\Omega^2 + 2\dot{S}_n T_n \Omega + \frac{1}{2}\left(\beta + \lambda\alpha_n^4\right)^2 S_n^2 + \dot{T}_n^2 + S_n^2\Omega^2 - 2\dot{T}_n S_n + \frac{1}{2}\left(\beta + \lambda\alpha_n^4\right)^2 T_n^2 + \dot{T}_n T_n\left(\beta + \lambda\alpha_n^4\right) \\ &\quad + (e\alpha_n^2 - f_0)\alpha_n^2(S_n^2 + T_n^2)\bigg]\kappa_n + (\dot{S}_n^2 + \dot{T}_n^2)\left(\beta + \lambda\alpha_n^4\right) + 2\beta\Omega(\dot{S}_n T_n - S_n\dot{T}_n) \\ &\quad + \left[(\beta e - \lambda\Omega^2)\alpha_n^4 + \lambda(e\alpha_n^2 - f_0)\alpha_n^6 - \beta f_0\alpha_n^2 + \beta\Omega^2\right](S_n^2 + T_n^2) \geqslant 0 \end{aligned} \tag{23}$$

After some reduction we obtain the auxiliary matrix of the quadratic form

$$\begin{bmatrix} a & b & 0 & d \\ b & c & -d & 0 \\ 0 & -d & a & b \\ d & 0 & b & c \end{bmatrix} \tag{24}$$

where

$$a = \beta + \lambda\alpha_n^4 + \kappa_n, \quad b = \frac{1}{2}\left(\beta + \lambda\alpha_n^4\right)\kappa_n, \quad d = \Omega(\beta + \kappa_n),$$

$$c = \kappa_n\left[\alpha_n(e\alpha_n^2 - f_0) + \Omega^2 + \frac{1}{2}\left(\beta + \lambda\alpha_n^4\right)^2\right] + (e\alpha_n^2 - f_0)(\lambda\alpha_n^4 + \beta) - \Omega^2(\lambda\alpha_n^4 - \beta)$$

We recall the Sylvester's conditions for the positive-definiteness of the auxiliary matrix (24):

$$a > 0 \tag{25}$$

$$ac - b^2 > 0 \tag{26}$$

$$a(ac - b^2 - d^2) > 0 \tag{27}$$

$$(b^2 + d^2 - ac)^2 > 0 \tag{28}$$

As the latest inequality, (28) is satisfied, it is easy to notice that the third Sylvester inequality (27) is essential from the stability point of view. After extensive but straightforward algebra we obtain the quadratic inequality with respect to κ_n

$$\kappa_n^2 + 2\alpha_n^2(e\alpha_n^2 - f_0)\kappa_n + 4\frac{(\beta + \lambda\alpha_n^2)^2(e\alpha_n^2 - f_0)\alpha_n^2 - \Omega^2\lambda^2\alpha_n^8}{(\beta + \lambda\alpha_n^2)^2 + 4\alpha_n^2(e\alpha_n^2 - f_0)} \geqslant 0 \tag{29}$$

It leads to the determination of the value of κ_n and to the formula which determines χ_n

$$\chi_n = \frac{\sqrt{(\beta + \lambda\alpha_n^4)^4 + 4\Omega^2\lambda^2\alpha^8}}{\sqrt{(\beta + \lambda\alpha_n^4)^2 + 4\alpha_n^2(e\alpha_n^2 - f_0)}} - \lambda\alpha_n^4 \tag{30}$$

Estimating the limit behavior of χ_n as n tends to ∞, we find

$$\Omega^2 < \omega_1^2\left(1 + \beta\ell^4/\lambda\pi^4\right)^2(1 - f_0/f_{\mathrm{cr}}) \tag{31}$$

where $\omega_1 = \pi^2\sqrt{e}/l^2$ denotes the first natural frequency of the shaft at rest in the absence of axial force. Thus, Ω becomes larger if $f_0 < 0$, (i.e., f_0 is tensile force). We may observe that if $f_0 = f_{cr} = e\pi^2/l^2$ then $\Omega = 0$. It is evident that the critical angular velocity decreases as the inner damping coefficient λ increases.

4. Stability analysis of the shaft compressed by a time-dependent force

For a stationary continuous with probability one axial force the time derivative of the functional is calculated in the same way as for the constant axial force. The constant χ in inequalities (10) and (11) is a random functions due to the randomness of f. Substituting

$$b \to b - \alpha_n^2 f(t)$$

$$c \to c - (\beta + \lambda\alpha_n^4)\alpha_n^2 f(t)$$

we obtain the matrix of which the positive definiteness implies the stochastic stability of the shaft motion. Using the Sylvester's conditions yields the modified value of the function χ_n

$$\chi_n = \frac{\sqrt{(\beta + \lambda\alpha_n^4)^4 + 4[(\beta + \lambda\alpha_n^4)^2 + \alpha_n^2 f(t)]\alpha_n^2 f(t) + 4\Omega^2\lambda^2\alpha^8}}{\sqrt{(\beta + \lambda\alpha_n^4)^2 + 4\alpha_n^2(e\alpha_n^2 - f_0)}} - \lambda\alpha_n^4 \tag{32}$$

The ergodicity of the axial force leads to the following almost sure stochastic stability condition

$$\mathbf{E} \max_n \chi_n(t) \leqslant \beta \tag{33}$$

where **E** denotes a mean value operator. Since χ depends on β, the almost sure stability criterion has a form of the transcendental equation involving the force statistical characteristics. In order to obtain the stability regions we choose discrete values of f and compute χ_n from Eq. (32). We select the largest value corresponding to the given value of f. Then we multiply it by the density of probability distribution depending on the variance of axial force f and we integrate over the range of f. This procedure is performed for unactivated and activated states and for the varying damping coefficient β until the inequality (33) holds.

5. Results

Numerical calculations based on the formula (33) are performed for changing parameters of SMA fibers and external damping coefficient. A number of iterative steps are performed in order to determine the value of β. The dimensions of the hybrid shafts are taken as: length $\ell = 1$ m, radius $r = 0.04$ m, and total thickness $h = 0.002$ m. Stochastic stability domains are calculated for the fixed shaft angular velocity $\Omega = 500$ 1/s smaller than the critical value obtained from Eq. (31) and the constant component of external axial force equal to zero. The material data are given in Table 1. The shaft consists of seven layers of equal thickness: of two external activated layers with the SMA fibers parallel to the shaft axis and of five internal conventional layers symmetrically arranged with the lamination angle Θ. Thus, the laminate configuration can be uniquely defined by the following notation: $[0°/\Theta/-\Theta/\Theta/-\Theta/\Theta/0°]$. Expressing the in-plane stiffnesses of lamina by the engineering constants we can calculate the in-plane stiffnesses A_{ij}

Table 1
SMA hybrid shaft specifications

Material	Nitinol–Epoxy NiTi – 40%, Epoxy – 60%		Glass–Epoxy	Graphite–Epoxy
	Activated	Unactivated		
Density kg/m^3	2350	2350	1790	1560
E_{11} GPa	41.93	19.31	53.98	211.0
E_{22} GPa	20.93	17.25	17.93	5.30
G_{12} GPa	7.54	6.43	8.96	2.60
ν_{12}	0.25	0.25	0.25	0.25
λ	0.01	0.019	0.01	0.01

$$A_{ij} = \left(\frac{5}{7}\bar{Q}_{ij} + \frac{2}{7}Q_{ijNiTi}\right)h, \quad i,j = 1,2 \tag{34}$$

where $\bar{Q}_{ij}$ represent the transformed in-plane stiffnesses of conventional lamina depending on angle Θ, Q_{ijNiTi} are in-plane stiffnesses of the lamina with SMA fibers (the lamination angle is equal to zero). Substituting Eq. (34) into Eq. (2) we obtain the reduced Young's modulus E_0 of the beam-like cylindrical shell for both the unactivated and the activated state of SMA fibers. The maximum recovery stress corresponding to the initial strain $\epsilon = 1\%$ was assumed in calculations. While calculating the axial force f_0 in the activated state we assume that the recovery stresses are partially acting in the cross-section of the shaft and partially are balanced by the boundaries. The ratio of the force balanced by the edges to the total recovery force is called the boundary recovery ratio and is denoted by r_b. The extremum states $r_b = 1$ when the recovery stresses are balanced totally by the boundaries, and $r_b = 0$ when the recovery stresses are balanced by the reminder of the shaft cross-section, are shown in Fig. 2. The results are shown in Figs. 3–6. The

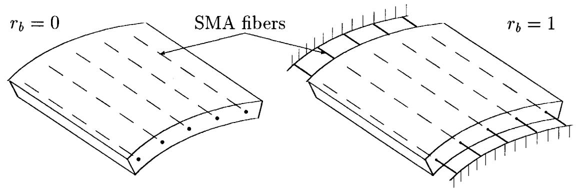

Fig. 2. Visualization of boundary conditions.

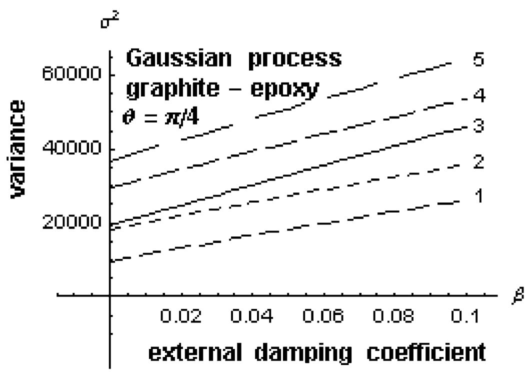

Fig. 3. Comparison of stochastic stability domains for unactivated and activated nitinol–epoxy/graphite–epoxy shaft for different activation factors.

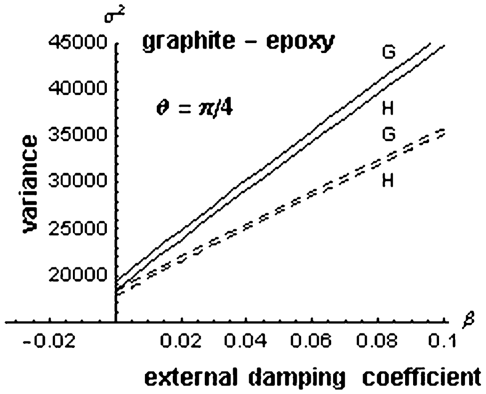

Fig. 4. Critical value of force variance as a function of the external damping coefficient β for different class of excitation.

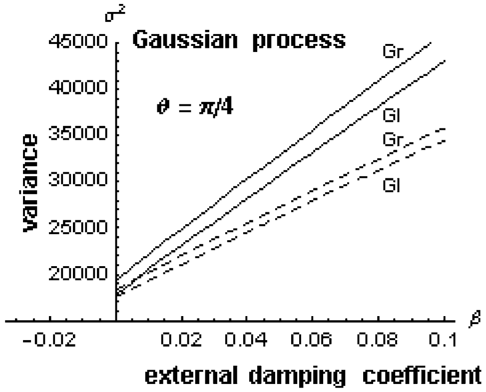

Fig. 5. Critical value of force variance as a function of the external damping coefficient β for different shaft materials.

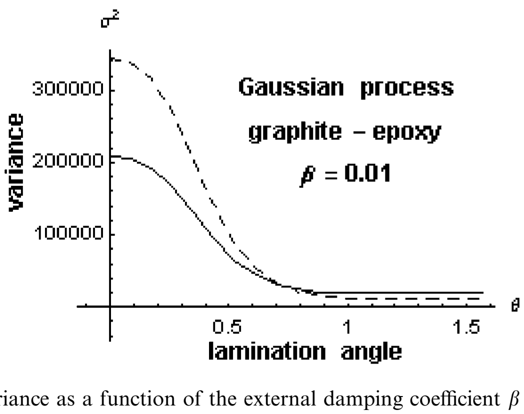

Fig. 6. Critical value of force variance as a function of the external damping coefficient β for various lamination angles Θ.

influence of different activation parameters on stability domains of hybrid graphite–epoxy/nitinol–epoxy shaft with the Gaussian parametric excitation is shown in Fig. 3. Curves 1–5 represent the stability limits: curve 1 is for activated state due to decrease of the inner damping coefficient λ only; curve 2 is for the unactivated state; curve 3 is for fully activated state, $r_b = 1$; curve 4 is for the activated state with no decrease of inner damping coefficient λ and for no recovery axial force, $r_b = 0$; curve 5 is for the activated state with no decrease of inner damping coefficient λ, $r_b = 1$. It is seen that among three thermal activation factors: the increase of the effective Young's modulus, the increase of extensional axial force, and the decrease of internal damping, the greatest role in the increase of the stability domain plays the axial force. In contradiction to the formula (31) (for the constant external axial force) the decrease of internal damping significantly decreases the stability domains. The largest stability domains occur when the recovery stresses are balanced totally by the boundaries ($r_b = 1$). Figs. 4–6 compare the critical value of force variance σ^2 as a function of the external damping coefficient β for different class of parametricexcitation, materials, and lamination angles Θ, respectively. The activated states and the unactivated states are denoted by continuous and broken lines, respectively. Fig. 4 compares the stability domains on plane (β, σ) calculated for the nitinol–epoxy/graphite–epoxy shaft ($\Theta = \pi/4$) in unactivated and activated states for the Gaussian (G) and harmonic forces (H). The critical variance of time-dependent force component strongly depends on the external damping coefficient β. The differences between stability regions calculated for the Gaussian loading and the harmonic are negligible. The influence of the shaft material on the critical value of force variance is shown in Fig. 5, where the nitinol–epoxy/graphite–epoxy shaft and the nitinol–epoxy/glass–epoxy shaft ($\Theta = \pi/4$) are denoted by Gr and Gl, respectively. The influence of lamination angle on stability domain is calculated for the external damping with $\beta = 0.01$.

6. Conclusions

A technique has been presented for the analysis the dynamic stability of a globally activated simply supported hybrid shaft consisting of the symmetrically laminated classical angle-plies and the symmetrically laminated active plies with axially oriented SMA fibers. The dynamic stability and the stochastic stability problem is reduced to the problem of the positive definiteness of the auxiliary matrix. The explicit criteria derived in the paper define stability regions in terms of the geometrical and material properties, the lamination angle, as well as the constant values and variance of axial loading. For the constant axial force the criterion assumes a closed form of an algebraic inequality. If the axial force is time-dependent, the almost sure stability criterion has a form of the transcendental equation involving the force probability distribution. Analytical results are presented to demonstrate how the thermal activation affects critical parameters. The results indicate that the global activation significantly increases the admissible variance of time-dependent component. The most important role in increasing of the stability domains is played by the axial force following from the recovery stresses. The increase depends highly on the boundary recovery ratio. The effect is more pronounced for the graphite–epoxy/nitinol–epoxy shell than for the glass–epoxy/nitinol–epoxy hybrid shafts. The influence of the loading class (Gaussian or harmonic) is not substantial.

Acknowledgements

The study was supported by the State Committee for Scientific Research (Grant KBN - No. 7T07C02211).

References

Bauchau, O.A., 1983. Optimal design of high speed rotating graphite/epoxy shafts. Journal of Composite Materials 17, 170–181.

Cross, W.B., Kariotis, A.H., Stimler, F.J., 1970. Nitinol characterization study. Goodyear Aerospace Corporation Report, No. Ger 14188 NASA CR-1433, Akron, Ohio.

Dejonghe, W., Delaey, L., De Baptist, R., Van Humbeck, J., 1977. Temperature- and amplitude-dependence of internal friction in Cu–Zn–Al alloys. Metal Science 11, 523–540.

Jones, R.M., 1975. Mechanics of composite materials. McGraw-Hill, Scripta Book Company, Washington.

Nepershin, R.I., Klimov, W.W., 1986. Optimal design of composite transmission shafts with respect to costs and weight. Mechanics of Composite Materials 4, 690–695 (in Russian).

Pietrzakowski, M., 2000. Natural frequency modification of thermally activated composite plates. Mécanique Industries 1 (3), 313–320.

Rogers, C.R., 1990. Active vibration and structural acoustic control of shape memory alloy hybrid composites: experimental results. Journal of the Acoustical Society of America 88, 2803–2811.

Rogers, C.A., Fuller, C.R., Liang, C., 1990. Active control of sound radiation from panels using embedded shape memory alloy fibers. Journal of Sound and Vibration 136, 164–170.

Schultz, A.B., Tsai, S.W., 1969. Measurements of complex dynamic moduli for laminated fiber-reinforced composites. Journal of Composite Materials 3, 434–443.

Tylikowski, A., 1986. Dynamic stability of visco-elastic continuous systems under time-dependent loading. Mechanika Teoretyczna i Stosowana 24, 127–137.